



NRC Publications Archive Archives des publications du CNRC

High-yield UV-photochemical vapor generation of iron for sample introduction with ICP-OES

Zheng, Chengbin; Sturgeon, Ralph E.; Brophy, Christine S.; He, Shaopan; Hou, Xiandeng

This publication could be one of several versions: author's original, accepted manuscript or the publisher's version. / La version de cette publication peut être l'une des suivantes : la version prépublication de l'auteur, la version acceptée du manuscrit ou la version de l'éditeur.

For the publisher's version, please access the DOI link below. / Pour consulter la version de l'éditeur, utilisez le lien DOI ci-dessous.

Publisher's version / Version de l'éditeur:

<https://doi.org/10.1021/ac100059b>

Analytical Chemistry, 82, 7, pp. 2996-3001, 2010-03-11

NRC Publications Record / Notice d'Archives des publications de CNRC:

<https://nrc-publications.canada.ca/eng/view/object/?id=33219186-675a-4cd8-9c01-58813e99050a>

<https://publications-cnrc.canada.ca/fra/voir/objet/?id=33219186-675a-4cd8-9c01-58813e99050a>

Access and use of this website and the material on it are subject to the Terms and Conditions set forth at

<https://nrc-publications.canada.ca/eng/copyright>

READ THESE TERMS AND CONDITIONS CAREFULLY BEFORE USING THIS WEBSITE.

L'accès à ce site Web et l'utilisation de son contenu sont assujettis aux conditions présentées dans le site

<https://publications-cnrc.canada.ca/fra/droits>

LISEZ CES CONDITIONS ATTENTIVEMENT AVANT D'UTILISER CE SITE WEB.

Questions? Contact the NRC Publications Archive team at

PublicationsArchive-ArchivesPublications@nrc-cnrc.gc.ca. If you wish to email the authors directly, please see the first page of the publication for their contact information.

Vous avez des questions? Nous pouvons vous aider. Pour communiquer directement avec un auteur, consultez la première page de la revue dans laquelle son article a été publié afin de trouver ses coordonnées. Si vous n'arrivez pas à les repérer, communiquez avec nous à PublicationsArchive-ArchivesPublications@nrc-cnrc.gc.ca.



High-Yield UV-Photochemical Vapor Generation of Iron for Sample Introduction with ICP-OES

Chengbin Zheng^{a,b}, Ralph E. Sturgeon^{a*}, Christine S. Brophy^a, Shaopan He^b and Xiandeng Hou^{b*}

^a *Institute for National Measurements Standards, National Research Council Canada, Ottawa, Ontario, Canada, K1A 0R6.*

^b *College of Chemistry, Sichuan University, Chengdu, Sichuan, 610064, China.*

*Corresponding author. Fax: (613) 993-6395.

E-mail: Ralph.Sturgeon@nrc.ca (Ralph E. Sturgeon), Houxid@scu.edu.cn (Xiandeng Hou)

ABSTRACT

A novel approach to the generation of volatile iron compounds (likely the pentacarbonyl) with high efficiency is described wherein solutions containing either Fe^{2+} or Fe^{3+} and low molecular weight organic acids such as formic, acetic or propionic are exposed to a UV source. An optimum generation efficiency of $60 \pm 2 \%$ was achieved in 50 % formic acid at pH 2.5 with an irradiation time of 250 s by use of a 17 W low pressure mercury grid lamp. Compared to conventional solution nebulization, sensitivity and limit of detection were improved 80- and 100-fold, respectively, yielding 1620 cps per ng/ml and 0.025 ng/ml at the 238.204 nm Fe II emission line. A precision of 0.75 % RSD was achieved at a concentration of 100 ng/ml. Photochemical vapor generation sample introduction was used for the determination of trace iron in several environmental Certified Reference Materials, including National Research Council Canada DORM-3 fish muscle tissue, DOLT-3 and DOLT-4 fish liver tissues and SLRS-5 river water, providing analytical results in excellent agreement with certified values based on simple external calibration.

Keywords: photochemical vapor generation; volatile iron compounds; vapor sample introduction; inductively coupled plasma optical emission spectrometry.

INTRODUCTION

Despite its high crustal abundance (5.6 %, [1]), the determination of iron in many environmental and biological samples is challenging due to both low content and the presence of potentially troublesome concomitant matrix elements that perturb detector response. This is perhaps exemplified most acutely by the quantitation of dissolved iron in surface waters of the open ocean [2] where concentrations of 0.1 nM (6 ng/kg) are encountered, or the determination of iron isotope ratios in such samples [3]. The important role of iron in oceanic biogeochemistry drives such studies and has resulted in the development of numerous protocols for matrix separation, analyte preconcentration and detection in efforts to circumvent these obstacles. Co-precipitation [4] and solid phase extraction [5-7] have become principal approaches for matrix separation and preconcentration whereas inductively coupled plasma mass spectrometry (ICP-MS) appears as a most favored detector, considering that quantitation by isotope dilution may be undertaken and spectral interferences frequently resolved through use of a sector field instrument (medium resolution) [3] or collision cell technology and cold plasmas [8].

A completely different approach to potential alleviation of these problems can be realized through use of chemical vapor generation (CVG). Although practiced for almost 40 years as an effective alternative sample introduction technique for hydride forming elements [9], it is only recently that the scope of application of the classical tetrahydroborate reductant has been broadened to include a number of transition and noble metals [10]. However, apart from a single report by Rigin [11] nearly 20 years ago, CVG of volatile species of iron in sufficient yield for favorable analytical use has not

been realized. Fortunately, newer approaches to vapor generation based on radical induced alkylation and carbonylation [12, 13] have suggested iron may be amenable to such reactions.

We report here a novel approach to the high yield production of volatile iron species [presumably $\text{Fe}(\text{CO})_5$] by application of UV photochemical vapor generation (PVG) and its use for quantitation of iron in seawater and biological tissues. Efficient matrix separation and high generation efficiency serve to enhance limits of detection by inductively coupled plasma optical emission spectrometry (ICP-OES) more than 100-fold over conventional solution nebulization sample introduction.

EXPERIMENTAL

Instrumentation. An intermittent injection mode UV photochemical vapor generation (PVG) system was based on use of a four channel minipuls 2 peristaltic pump (Gilson, Middleton, WI) to deliver sample containing formic acid to a UV photo-reactor and evacuate waste from a gas-liquid separator. A schematic diagram of the UV-PVG system interfaced to a Perkin–Elmer Optima 3000 radial view ICP–OES operated at the Fe II 238.204 nm line is illustrated in Figure 1. The UV photo-reactor consisted of a 17.4 W low pressure UV mercury grid lamp (Analamp, Claremont, CA) onto which a quartz tube (25 cm \times 2.5 mm i.d. \times 3.5 mm o.d.; 5 mL internal volume), contoured to follow the discharge lamp geometry, was positioned. The photo-reactor was wrapped with aluminum foil which served to protect the operator as well as increase efficiency by reflecting UV radiation from the lamp back onto the sample. The unit was continuously

purged with a 2 L min^{-1} flow of Ar to prevent ozone formation. Two gas-liquid separators (GLS) were operated in tandem, the first adopted from a Tekran Instruments series 2600 automated water analysis system (Toronto, Canada) with the second being of conventional design (10 mL internal volume) but with the waste outlet sealed to prevent unwanted escape of analyte vapors. This second GLS was immersed in an ice bath to ensure no condensed liquid droplets were transported to the ICP. The nebulizer gas flow channel of the emission instrument was used to regulate an Ar carrier gas to transport the volatile iron species separated from liquid phase. A 75 cm length of poly(tetrafluoroethylene) (PTFE) tubing (2.5 mm i.d. \times 4.0 mm o.d) connected the outlet of the second GLS to the base of the ICP-OES torch. Operating parameters are summarized in Table 1.

Reagents and solutions. All solutions were prepared using 18 M Ω -cm deionized water (DIW) produced by reverse osmosis of tap water followed by deionization (Barnstead/Thermolyne Corp, Iowa, USA). Nitric, sulfuric and hydrochloric acids were purified in-house prior to use by sub-boiling distillation of reagent grade feedstock in a quartz still. High purity NaNO_3 , NaCl and Na_2SO_4 (Fisher Scientific) were used, except where indicated otherwise. Environmental grade ammonium hydroxide (20–22%, v/v), used for adjusting the pH of the reaction solution, was purchased from Anachemia Science (Montreal, PQ, Canada). A 1000 mg L^{-1} stock solution of Fe(III) was obtained from SCP science (Montreal, PQ, Canada). A 1000 mg L^{-1} Fe(II) stock solution was prepared from dissolution of high purity iron powder with sub-boiling distilled hydrochloric acid followed by dilution with boiled (deoxygenated) DIW. The solution

was then stored in a screw-capped polypropylene bottle securely sealed with PTFE tape in an effort to minimize any subsequent oxidation. Calibration solutions were prepared daily by dilution of iron stock solutions with low molecular weight (LWM) organic acids, including high purity formic (88%, GFS, Canada), analytical reagent grade formic (23 M, Anachemica), acetic (6.3 M, BDH) and propionic acids (13 M, BDH). Solutions were pH adjusted by addition of high purity ammonium hydroxide. High purity Ar was obtained from Praxair Products Inc. (Mississauga, ON, Canada).

Several environmental and biological Certified Reference Materials from the National Research Council Canada (NRCC), including DORM-3 (Fish protein), DOLT-3 (Dogfish Liver Tissue), DOLT-4 (Dogfish Liver Tissue) and SLRS-5 (River water), were used to validate the accuracy of the proposed methodology.

Analytical Procedure and sample preparation. Volatile iron compounds were generated when 5 mL aliquots of standard solutions of iron containing various LWM organic acids adjusted to pH 2.5 were introduced to the photo-reactor for a typical irradiation time of 250 s. The solutions were then flushed to the first GLS at a nominal flow rate of 1 mL min⁻¹ from which the gaseous products were separated from the liquid phase and then directed to the second GLS to remove any condensed water vapor. Volatile iron species were swept to the plasma and response detected at the 238.204 nm Fe II emission line.

Sample preparation was undertaken in a class-100 clean room. Test samples of nominal 0.25 g of CRMs DORM-3, DOLT-3 and DOLT-4 were weighed into pre-cleaned Teflon

digestion vessels (CEM ACV Type) and 7 mL HNO₃ and 200 µL (30%) H₂O₂ added. Samples blanks were processed along with the CRM samples. The vessels were capped and the contents digested using a microwave digestion system (CEM, Model MDS-2100). The digested samples were cooled and diluted to 25 mL final volume with DIW and stored in pre-cleaned polyethylene screw-capped bottles.

Safety precaution. The exact products produced in this system are as yet unidentified (likely iron carbonyl) but should be considered toxic. Essential safety precautions must be taken during all manipulations and an adequate ventilation/exhaust system used.

RESULTS AND DISCUSSION

PVG has recently proven to be not only an interesting laboratory curiosity, but a promising alternative to CVG for the practical determination of transition and noble elements as well as non-metals [12, 14-16]. As this is the first attempt at PVG of iron, it was necessary to undertake a full investigation of all physico-chemical parameters relating to generation and detection of the volatile species. This novel approach utilizes green organic acids combined with UV irradiation to substantially enhance generation efficiency while providing a tolerance to matrix interferences.

Optimization of PVG system and ICP-OES parameters. Initial experiments utilized a 1 m long 15 W Hg vapour lamp as the UV source and either continuously pumped the test solution through a 3 m length of 1.1 mm i.d PTFE tubing wrapped around the lamp, or through two 1 m long (2.5 mm i.d. × 3.5 mm o.d.) quartz tubes connected in series and

exposed to the length of the lamp. No response was achieved with the first arrangement, despite low solution flow rates to yield exposure times of up to 120 s, likely due to insufficient UV intensity as a consequence of the low transmission efficiency of the PTFE. A weak signal was detected with the second arrangement which increased with increased irradiation time, leading to the conclusion that enhanced PVG efficiency could likely be achieved by an intermittent flow injection mode whereby discrete sample volumes were introduced into the photo-reactor for predetermined irradiation times before sweeping the contents to the phase separators. When this approach was implemented with the grid lamp and a quartz tube capable of accommodating a 5 mL test sample, a more than 30-fold enhancement in response could be realized.

The overall efficiency of gas-liquid separation and vapor transport, analyte concentration in the carrier gas and its residence time in the plasma were significantly influenced by the carrier gas flow rate, as shown in Figure 2. A response plateau was obtained in the range 0.60 - 0.70 L min⁻¹. Lower flow rate resulted in inefficient separation of the analyte from the liquid phase and low efficiency of transport to the ICP; higher flow rate resulted in significant dilution of analyte in the carrier gas. A transport gas flow rate of 0.65 L min⁻¹ was selected for all further experiments.

Effect of LWM organic acids. A 100 µg L⁻¹ solution of Fe(III) was used to investigate the effect of concentration and nature of LWM organic acid on response. Formic, acetic and propionic acids were selected for study; results are depicted in Figure 3 and are similar to those reported earlier for PVG of nickel [14]. Although acetic and propionic acids can be used to generate a volatile iron species, their efficiencies are too low to be

useful for analytical purposes and formic acid was thus selected for all further studies. The most likely candidate for analytical species produced in this medium is $\text{Fe}(\text{CO})_5$. Low efficiencies in the presence of the other acids may be a consequence of the slower kinetics of generation of possible alkylated adducts of iron or their lower volatility and less complete phase separation once formed. Response increased significantly with increasing concentration of formic acid throughout the range 0 - 50% (v/v) followed by a plateau at higher concentrations. A 50% (v/v) formic acid medium was thus used for subsequent experiments. A large blank is obtained when reagent grade formic acid is used because it contains more than $200 \mu\text{g L}^{-1}$ of iron as a contaminant, necessitating use of sub-boil distilled reagent for this work.

Effect of irradiation time. The effect of irradiation time on response was investigated using $100 \mu\text{g L}^{-1}$ solutions of $\text{Fe}(\text{II})$ and $\text{Fe}(\text{III})$ under the optimized experimental conditions. Results are summarized in Figure 4a. In the absence of UV, no signal is detected. Moreover, the optimum irradiation time for iron, 250 – 350 s, is substantially longer than that required for elements such as As, Se, Hg, Co and Ni (typically < 120 s). With increased irradiation time, gaseous products such as iron carbonyl and carbon oxides accumulated as numerous expanding bubbles in the photo-reactor which pushed the test solution into the GLS prior to optimum exposure to the irradiation field. This resulted in a partial loss of sample and the signal thus decreased beyond a 350 s irradiation time. No difference in response from solutions of either $\text{Fe}(\text{II})$ or $\text{Fe}(\text{III})$ is evident when the irradiation time is longer than 225 s.

Increasing the temperature of the iron feed solution to 55° C (water bath heating) permitted a reduction in the optimum UV irradiation time to 120 s and thus an increase in potential sample throughput. In order to gain further insight into this effect, a micro-thermal couple (chromel-alumel) was inserted into the reaction solution through an in-line port to measure the change in temperature with increasing irradiation time (Figure 4 b). Temperature increased to 55° C after 120 s UV irradiation (Figure 4 b), which corresponded to the sharp increase in response beyond 100 s (Figure 4a), suggesting that the temperature is possibly the most important factor for PVG of iron and the first 100 s of irradiation time is primarily consumed with heating the reaction solution.

Effect of inorganic acids. Inorganic acids such as HCl, HNO₃ and H₂SO₄ are frequently used not only as reaction media for conventional CVG, but also as oxidizing/solubilizing agents for the preparation of samples. The effects of these acids on PVG response from iron are summarized in Figure 5a. In contrast to earlier investigated PVG systems for Ni and Se [14, 15], response unexpectedly sharply decreases, irrespective of the inorganic acid present. For Se [15], the PVG signal was not reduced even in the presence of 100 mM HCl or H₂SO₄. Results arising from substitution of NaCl, NaNO₃ and Na₂SO₄ for these acids in order to ascertain the impact of whether the anion or pH is responsible is shown in Figure 5b. With the exception of the nitrate anion, there are no noticeable effects on the generation efficiency, even at concentrations of 500 mM, leading to the conclusion that signal suppression arises primarily because of changes in the pH. Further studies utilizing addition of sodium formate or acetate to the 50 % (v/v) formic acid present in the sample solution in an effort to adjust (buffer) the pH gave rise to a 40-fold enhancement in the generation efficiency at concentrations of 2 M. Unfortunately, these

salts cannot be used in practice because they contain high levels of iron impurities. Environmental grade ammonium hydroxide (containing $<10 \text{ ng L}^{-1}$ iron) can be used for this purpose and provides the same signal enhancement at pH 2.5. Additional experiments utilizing 5 M sodium formate as the generation medium in lieu of formic acid as the source of $[\text{HCOO}^-]$ were undertaken to further establish the optimal pH for PVG by addition of HCl for its adjustment. Figure 6 reveals the optimum pH range to be 2.0 ~ 3.0. It is speculated that the mechanism for PVG may involve an initial reduction of ionic iron to free atoms in solution with concurrent generation of and attack by organic radicals. The resultant volatile iron species subsequently transfers to the gas phase. Low generation efficiency may arise if the reaction occurs in a medium which is too acidic, as re-dissolution of iron may immediately occur, or if the solution is too basic, as the metal hydroxide may form.

Generation efficiency. The net efficiency was estimated from a comparison of the relative concentrations of analyte in the feed and waste solutions after the sample was subjected to PVG. For this purpose, a $500 \text{ } \mu\text{g L}^{-1}$ feed solution of either Fe(II) or Fe(III) was used and the waste solution collected in a pre-cleaned container. The concentration of iron in both solutions was then determined by the method of standard additions using conventional solution nebulization. As test solutions containing 50 % formic acid cannot be directly introduced into the ICP without extinguishing the plasma, they were diluted 4-fold with DIW prior to analysis. Without prior pH adjustment, efficiency was estimated to be in the range 1~2 % when the reaction medium consisted of only 50 % (v/v) formic acid. A series of standard solutions ($50 - 5000 \text{ } \mu\text{g L}^{-1}$ iron) containing 50 % formic acid

adjusted to pH 2.5 with ammonium hydroxide were used to further investigate PVG efficiency. Elevated test concentrations were required as otherwise unreliable data were generated because the levels ($< 100 \mu\text{g L}^{-1}$) are too close to the limit of detection obtained with conventional solution nebulization. This is illustrated in Figure 7, wherein it is clear that reliable estimates of $60 \pm 2 \%$ efficiency are obtained for higher test concentrations adjusted to the optimum pH. The efficiency estimated in this manner is consistent with the enhanced sensitivities (80-fold increase in slope of calibration curve) arising from PVG sample introduction compared to conventional solution nebulization.

Interferences. Whereas a major shortcoming associated with conventional hydride generation is the serious interferences arising from transition and noble metal ions, PVG is remarkably less afflicted. Guo *et al.* [17] reported no interference from the presence of $500 \text{ mg L}^{-1} \text{Ni}^{2+}$ and $100 \text{ mg L}^{-1} \text{Co}^{2+}$ during PVG of selenium. However, in the presence of $10 \text{ mg L}^{-1} \text{Ni}^{2+}$ or Co^{2+} , serious signal suppression is encountered for its conventional hydride generation [18]. The effects of 16 concomitant ions on the efficiency of PVG of iron are summarized in Table 2. No significant interferences from Ag^+ , Au^{3+} , Ca^{2+} , Cd^{2+} , Cu^{2+} , Hg^{2+} , Mg^{2+} , Pb^{2+} , Sn^{2+} and Zn^{2+} are evident, even at concomitant concentrations as high as 5 mg L^{-1} . However, several hydride-forming elements, particularly Se^{4+} and Te^{4+} , induced serious interference with PVG of iron from a $10 \mu\text{g L}^{-1}$ solution of Fe(III) . This likely arises because they are able to preferentially scavenge (react with) the UV-generated organic radicals. A further possibility is that the reduced Se or Te species may form an alloy or co-precipitate as a colloid [17] with the free iron atom intermediates generated during PVG. Such effects may potentially be eliminated or minimized when

rapid separation of volatile Se or Te species from the liquid phase can be accomplished. The anomalous significant positive interference from cobalt arises because of concurrent co-generation of its volatile species [19], giving rise to a spectral interference from a broadened close-lying Co II emission line at 237.862 nm which could be alleviated by use of the alternative Fe II 259.940 nm analytical line for detection.

Figures of merit. Table 3 summarizes analytical figures of merit achieved when using PVG for sample introduction and compares performance with that of several other analytical methods. Figure 8 illustrates typical calibration curves obtained for Fe(II) and Fe(III) using the optimized technique, characterized by the following calibration functions: $I_{\text{Fe(II)}} = 1618.8 C_{\text{Fe(II)}} - 9675$ and $I_{\text{Fe(III)}} = 1610.8 C_{\text{Fe(III)}} - 4626$ for Fe(II) and Fe(III), respectively, where C is the concentration ($\mu\text{g L}^{-1}$). Linear correlation coefficients are better than 0.99 in both cases and there is no significant difference in the efficiency of generation due to oxidation state. Linear range can be extended to higher than 10 mg L^{-1} and is limited by saturation of the detector. Precision of replicate measurement, expressed as a relative standard deviation (RSD, $n = 11$) is better than 0.75% at a concentration of $100 \mu\text{g L}^{-1}$. The LOD, defined as the analyte concentration equivalent to $3s$ (standard deviation) of 11 repeated measurements of a blank solution, is $0.025 \mu\text{g L}^{-1}$, some 40-fold better than that achieved with solution nebulization and competitive with ICP-MS detection.

Analysis of Certified Reference Materials. Several National Research Council Canada Certified Reference Materials were analyzed to validate the accuracy of the proposed

method. Direct PVG of iron in these samples was not successful because of serious interferences from the high residual concentration of nitric acid used for digestion of the biological tissues or sample preservation for the river water. Two approaches were used to overcome this problem for biological samples: 25 μ L aliquots of digests of DORM-3, DOLT-3 and DOLT-4 were diluted to 25 mL using 50 % formic acid and ammonium hydroxide to adjust the pH to 2.5; or 250 μ L aliquots of sample digest was evaporated to near dryness on a hot plate in a class 100 clean hood and reconstituted to 25 mL using 50 % formic acid and ammonium hydroxide to adjust the pH to 2.5. Due to the low concentration of Fe present in SLRS-5 river water, 10 mL aliquots were evaporated to near dryness and then diluted to 50 mL using 50 % formic acid and ammonium hydroxide to adjust the pH to 2.5. Analytical results are summarized in Table 4 for calibration based on external standards prepared in 50 % formic acid adjusted to pH 2.5 with ammonium hydroxide. No significant differences are evident between the obtained and certified values.

CONCLUSIONS

Highly efficient generation of volatile species of iron is achieved in the presence of formic acid by the action of UV light. This novel analytical methodology based on PVG provides an extremely sensitive, simple and reliable green technology for the determination of ultratrace concentrations of iron. The substantial enhancement in the LOD as a consequence of enhanced sample introduction efficiency will be further examined when coupled to ICP-MS as interferences often arising from $^{40}\text{Ca}^{16}\text{O}^+$ and $^{40}\text{Ar}^{16}\text{O}^+$ at m/z 56 may be significantly minimized because of efficient elimination of matrix together with “cold plasma” conditions. Application of isotope dilution calibration

techniques should lead to enhanced accuracy. Finally, it remains to explore the potential of PVG for the direct determination of iron in organic reagents with plasma based detection techniques.

ACKNOWLEDGMENTS

C. B. Zheng and X. D. Hou thank the National Natural Science Foundation of China (No.20835003 and No.20805032) for partial financial support of this project. C. B. Zheng is grateful to the NRCC for financial support while in Canada.

REFERENCES

1. S.R. Taylor, *Geochim. Cosmochim. Acta*, 28 1273 – 1285 (1964).
2. E.P. Achterberg, T.W. Holland, A.R. Bowie, R.F.C. Mantoura and P.J. Worlfsfold, *Anal. Chim. Acta*, 442, 1-14 (2001).
3. I. Petrov and C. Quetel, *J. Anal. At. Spectrom.*, 20, 1095 – 1100 (2005).
4. I. Petrov, C. Quetel and P.D.P. Taylor, *J. Anal. At. Spectrom.*, 22, 608 – 615 (2007).
5. H. Obata, H. Karatani, M. Matsui and E. Nakayama, *Mar. Chem.*, 56, 97- 106 (1997).
6. V. Camel, *Spectrochim. Acta, Part B*, 58, 1177 - 1233 (2003).
7. S. Nakashima, R.E. Sturgeon, S.N. Willie and S.S. Berman, *Fresenius' Z. Anal. Chem.* 330, 592 - 595 (1988).
8. F. Vanhaecke, L. Balcaen, G.D. Wannemacker and L. Moens, *J. Anal. At. Spectrom.*, 17, 933-943 (2002).
9. *Hydride Generation Atomic Absorption Spectrometry*, J. Dedina and D.L. Tsalev (Eds.), Wiley, New York, 1995
10. R. E. Sturgeon and Z. Mester, *Appl. Spec.*, 56, 202A-213A (2002)
11. V. Rigin, *Anal. Chim. Acta*, 283, 895-901(1993)
12. Y. He, X. Hou, C. Zheng and R.E Sturgeon, *Anal. Bioanal. Chem.* 388, 769 - 774 (2007)
13. X.-M. Guo, R.E. Sturgeon, Z. Mester and G.J. Gardner, *Anal. Chem.*, 76, 2401-2405 (2004).
14. C.B. Zheng, R.E. Sturgeon and X.D. Hou, *J. Anal. At. Spectrom.*, 24, 1452-1458 (2009).
15. C.B. Zheng, L. Wu, Q. Ma, Y. Lv and X.D. Hou, *J. Anal. At. Spectrom.*, 23, 514-520 (2008).
16. P. Grinberg and R.E. Sturgeon, *Spectrochim. Acta, Part B*, 64, 235 - 241 (2009).
17. X.-M. Guo, R.E. Sturgeon, Z. Mester and G.J. Gardner, *Anal. Chem.*, 75, 2092-2099 (2003).
18. P. Pohl and W. Zyrnicki, *Anal. Chim. Acta*, 468, 71-79 (2002).

19. P. Grinberg, Z. Mester, R.E. Sturgeon and A. Ferretti, *J. Anal. At. Spectrom.* 23, 583 - 587 (2008).
20. M. Segura, Y. Madrid, and C. Cámara, *J. Anal. At. Spectrom.*, 18, 1103-1108 (2003).
21. C.V.S. Ieggli, D.Bohrera, P.C. do Nascimento, L.M. de Carvalho and S.C. Garcia, *Talanta*, 80, 1282-1286 (2010)..

Table 1. ICP-OES parameters

| | UV-PVG-ICP-OES | Solution nebulization ICP-OES |
|--|----------------|----------------------------------|
| RF power, W | 1250 | 1250 |
| Nebulizer argon flow rate, L min ⁻¹ | 0.65 | 0.8 |
| Plasma argon flow rate, L min ⁻¹ | 15 | 15 |
| Auxiliary argon flow rate, L min ⁻¹ | 0.5 | 0.5 |
| Sample flow rate, mL min ⁻¹ | 2.9 | 1.5 |
| Viewing height, mm | 15 | 15 |
| Stabilization time, s | 15 | 15 |
| Analytical line, nm | 238.204 | 238.204 |

Table 2 Influence of concomitant ions on recovery of response from iron

| Test species | [Mn ⁺], µg L ⁻¹ | [M ⁺]/[Fe ³⁺] | Recovery, % ^a |
|--------------|--|---------------------------------------|--------------------------|
| Ag(I) | 5000 | 500 | 85 |
| As(III) | 500 (1000) | 50 (100) | 104 (68) |
| Au(III) | 5000 | 500 | 118 |
| Bi(III) | 500 (1000) | 50 (100) | 97 (60) |
| Ca(II) | 5000 | 500 | 98 |
| Cd(II) | 5000 | 500 | 89 |
| Cu(II) | 5000 | 500 | 80 |
| Co(II) | 5000 | 500 | 195 ^b |
| Hg(II) | 5000 | 500 | 102 |
| Mg(II) | 5000 | 500 | 99 |
| Ni(II) | 1000 (5000) | 100 (500) | 86 (40) |
| Pb(II) | 5000 | 500 | 112 |
| Se(IV) | 100 (500) | 10 (50) | 85 (40) |
| Sn(II) | 1000 (5000) | 100 (500) | 108 (60) |
| Te(IV) | 100 (500) | 10 (50) | 84 (36) |
| Zn(II) | 5000 | 500 | 87 |

^a10 µg L⁻¹ Fe(III) solution: mean recovery with typical precision of 10 % expressed as RSD. ^bApparent enhancement due to concomitant generation of volatile Co species and detection at an adjacent unresolved Co II emission line at 237.862 nm.

Table 3. Comparison of performance with other methodologies

| Method | Sensitivity cps/ $\mu\text{g L}^{-1}$ | RSD (Concentration), % | LOD, | reference |
|------------------------------------|--|-----------------------------------|----------------------------|-----------|
| PVG-ICP-OES pH 2.5 | 1620 | 0.75 ($100 \mu\text{g L}^{-1}$) | $0.025 \mu\text{g L}^{-1}$ | This work |
| PVG-ICP-OES no pH adjustment | 40 | 0.60 ($500 \mu\text{g L}^{-1}$) | $1.2 \mu\text{g L}^{-1}$ | This work |
| Conventional ICP-OES | 20 | 0.50 ($500 \mu\text{g L}^{-1}$) | $2.5 \mu\text{g L}^{-1}$ | This work |
| ICP-MS | | 3 ($100 \mu\text{g L}^{-1}$) | $0.74 \mu\text{g L}^{-1}$ | 20 |
| Flame AAS | | 3.5 ($112 \mu\text{g g}^{-1}$) | $70 \mu\text{g L}^{-1}$ | 21 |

Table 4. Determination of iron in Certified Reference Materials

| Sample treatment | Sample | Found ^a , mg kg ⁻¹ | Certified, mg kg ⁻¹ |
|--|--------|---|-----------------------------------|
| direct analysis after 1000-fold dilution | DORM-3 | 348 ± 71 | 347 ± 30 |
| | DOLT-3 | 1554 ± 114 | 1484 ± 57 |
| | DOLT-4 | 1825 ± 138 | 1833 ± 75 |
| evaporated to near dryness, reconstituted before analysis | DORM-3 | 337 ± 21 | 347 ± 30 |
| | DOLT-3 | 1559 ± 69 | 1484 ± 57 |
| | DOLT-4 | 1871 ± 87 | 1833 ± 75 |
| | SLRS-5 | 86.3 ± 6.3 ^b | 91.2 ± 5.8 ^b |
| ^a mean and standard deviation of results (n=3); ^b µg L ⁻¹ | | | |

Figures and Captions

Figure 1. Schematic diagram of the experimental set-up.

Figure 2. Effect of carrier gas flow rate on the responses from $100 \mu\text{g L}^{-1}$ Fe(III).

Figure 3. Effect of LWM organic acid on the response from $100 \mu\text{g L}^{-1}$ Fe(III): \square formic acid, O acetic acid, Δ propionic acid.

Figure 4. a) Effect of irradiation time on response from $100 \mu\text{g L}^{-1}$ Fe as: \square Fe(II) and O Fe(III).
(b) effect of irradiation time on temperature of the reaction solution.

Figure 5. a) Effect of inorganic acid on response from $100 \mu\text{g L}^{-1}$ Fe(III): \square HCl, O H_2SO_4 , Δ HNO_3 ; (b) effect of inorganic salts on response from $100 \mu\text{g L}^{-1}$ Fe(III): \square NaCl, O Na_2SO_4 , Δ NaNO_3 .

Figure 6. Effect of pH on the response from $100 \mu\text{g L}^{-1}$ Fe(III) in 50 % (v/v) formic acid.

Figure 7. Efficiency of vapor generation.

Figure 8. Typical calibration curves using PVG-ICP-OES obtained with \square Fe(II) and O Fe(III).

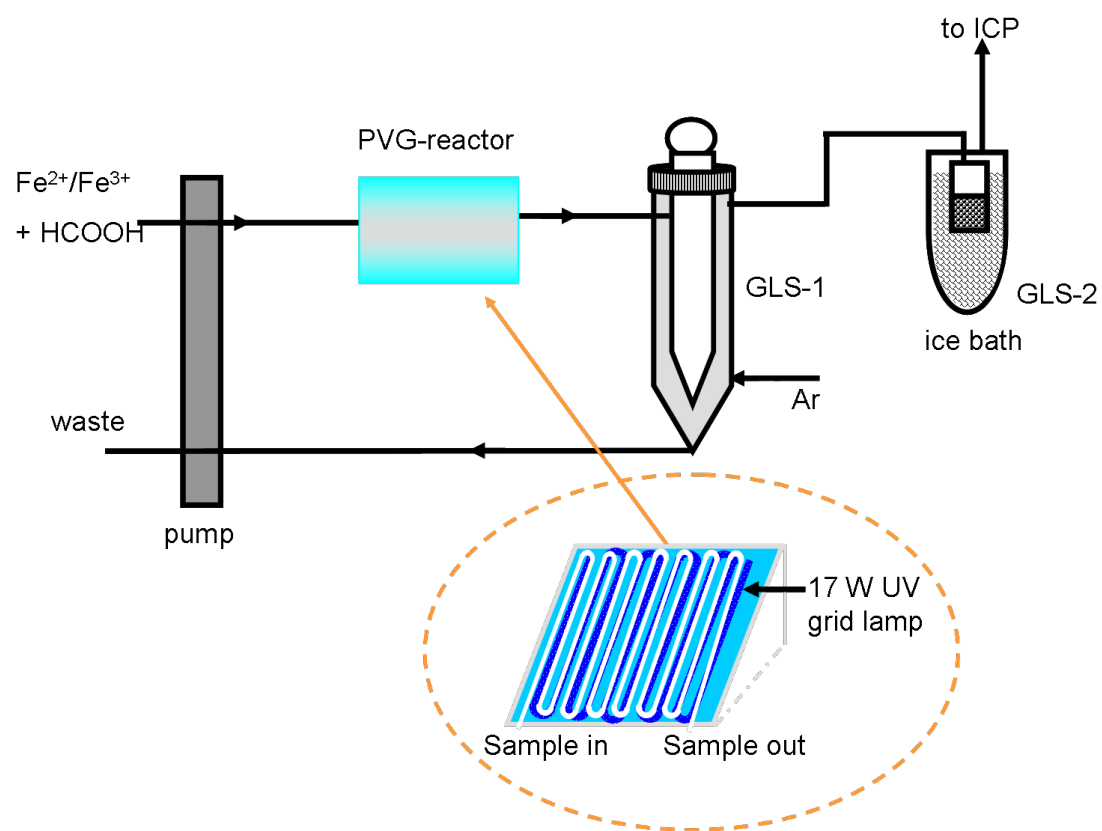


Figure 1. Schematic diagram of the experimental set-up.

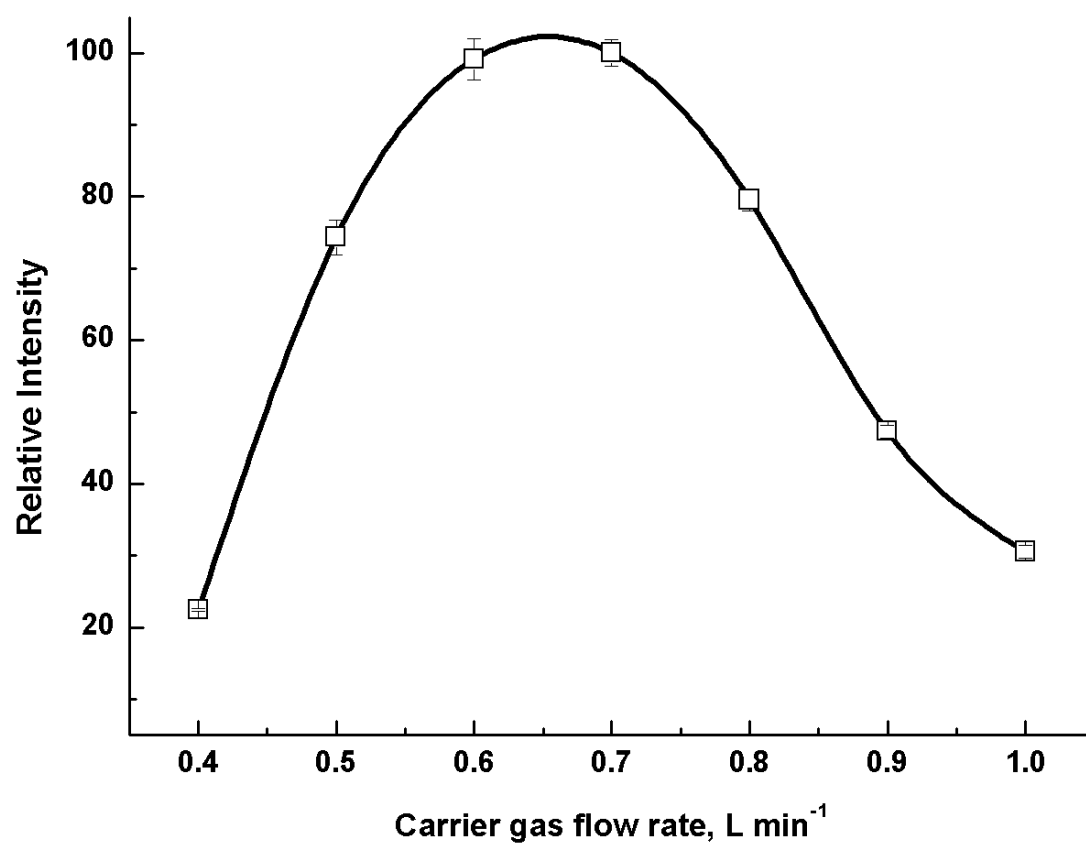


Figure 2. Effect of carrier gas flow rate on the responses from 100 $\mu\text{g L}^{-1}$ Fe(III).

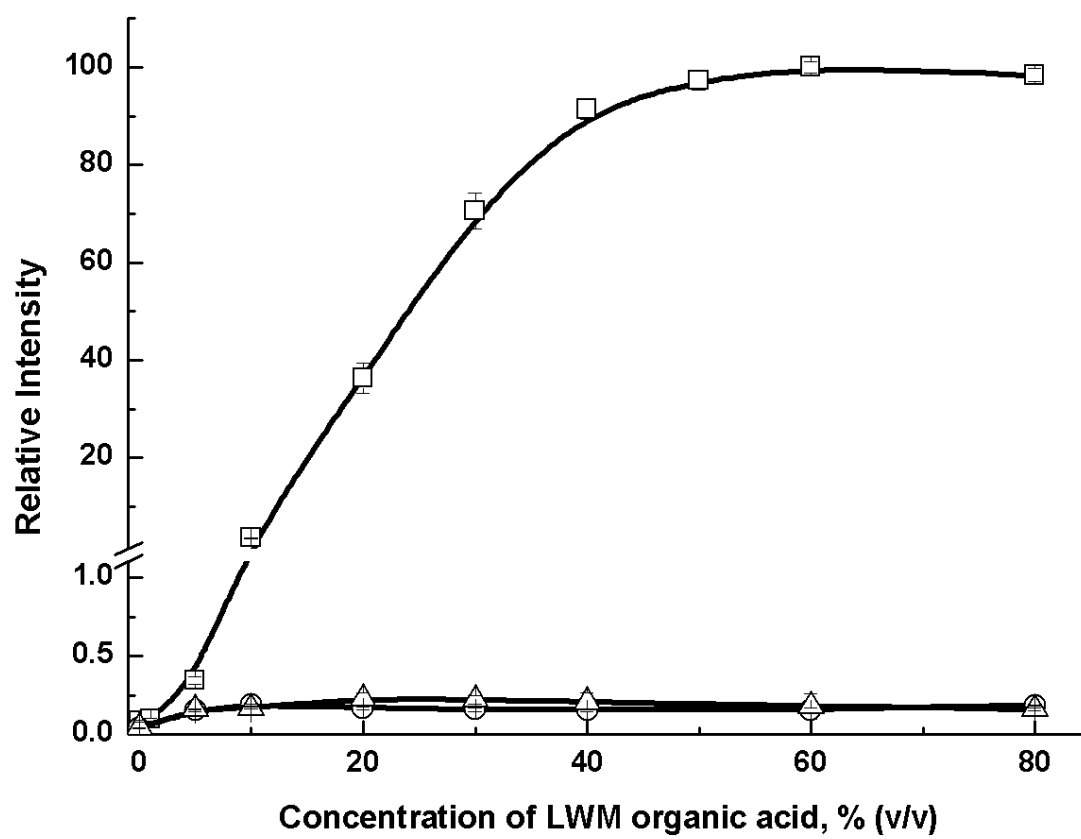


Figure 3. Effect of LWM organic acid on the responses from $100 \mu\text{g L}^{-1}$ Fe(III): □ formic acid, ○ acetic acid, and Δ propionic acid.

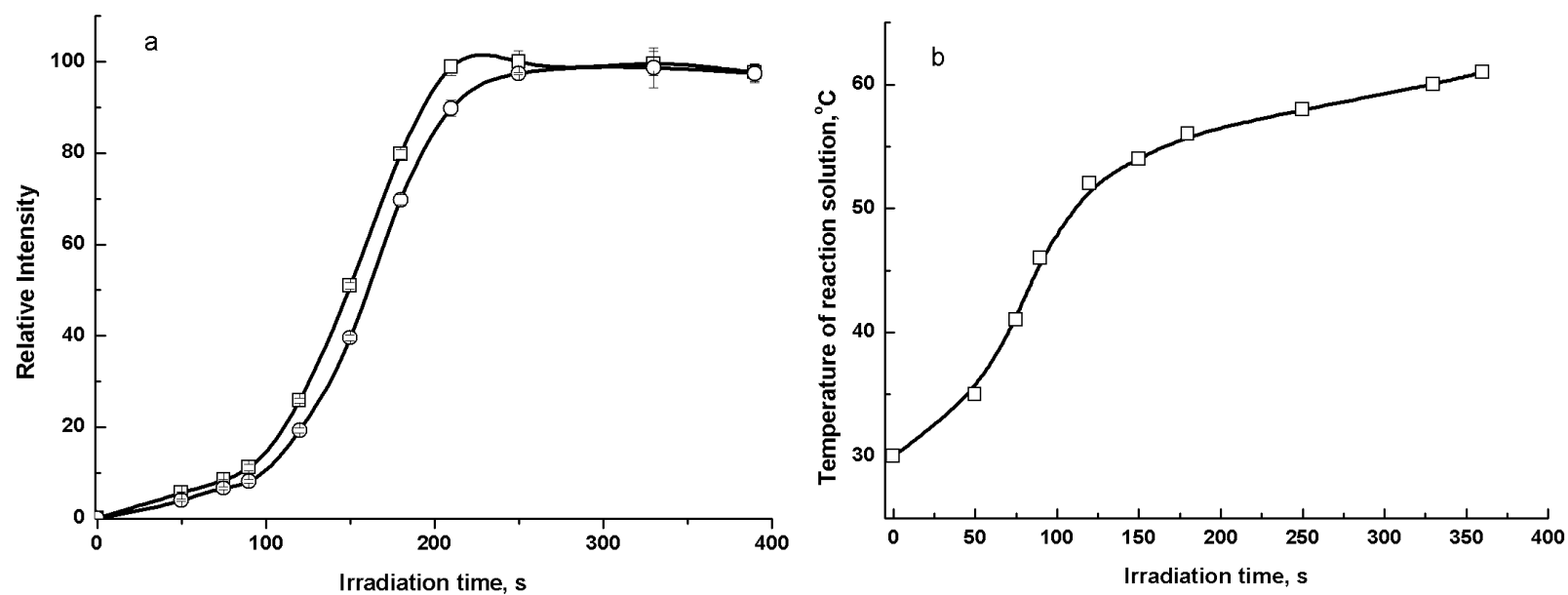


Figure 4. a) Effect of irradiation time on response from $100 \mu\text{g L}^{-1}$ Fe as: \square Fe(II) and \circ Fe(III).

(b) effect of irradiation time on temperature of the reaction solution.

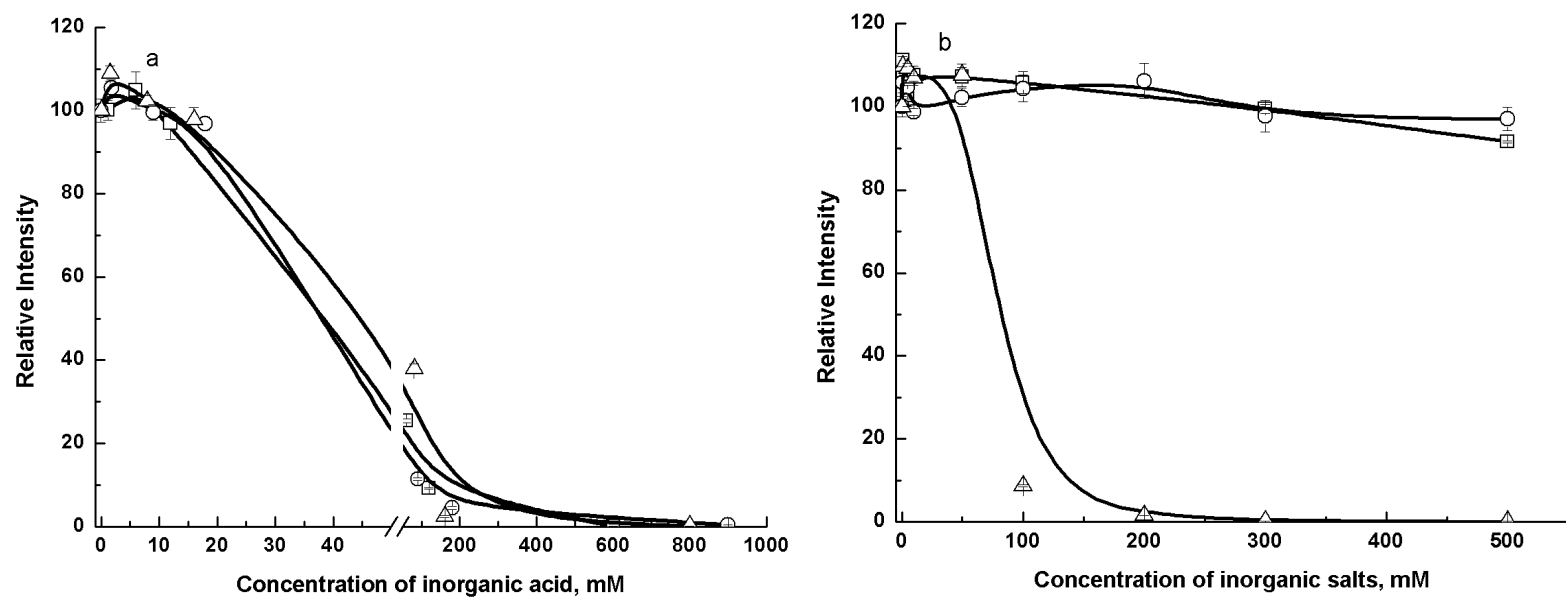


Figure 5. a) Effect of inorganic acid on response from 100 µg L⁻¹ Fe(III): □ HCl, ○ H₂SO₄, △ HNO₃; (b) effect of inorganic salts on response from 100 µg L⁻¹ Fe(III): □ NaCl, ○ Na₂SO₄, △ NaNO₃.

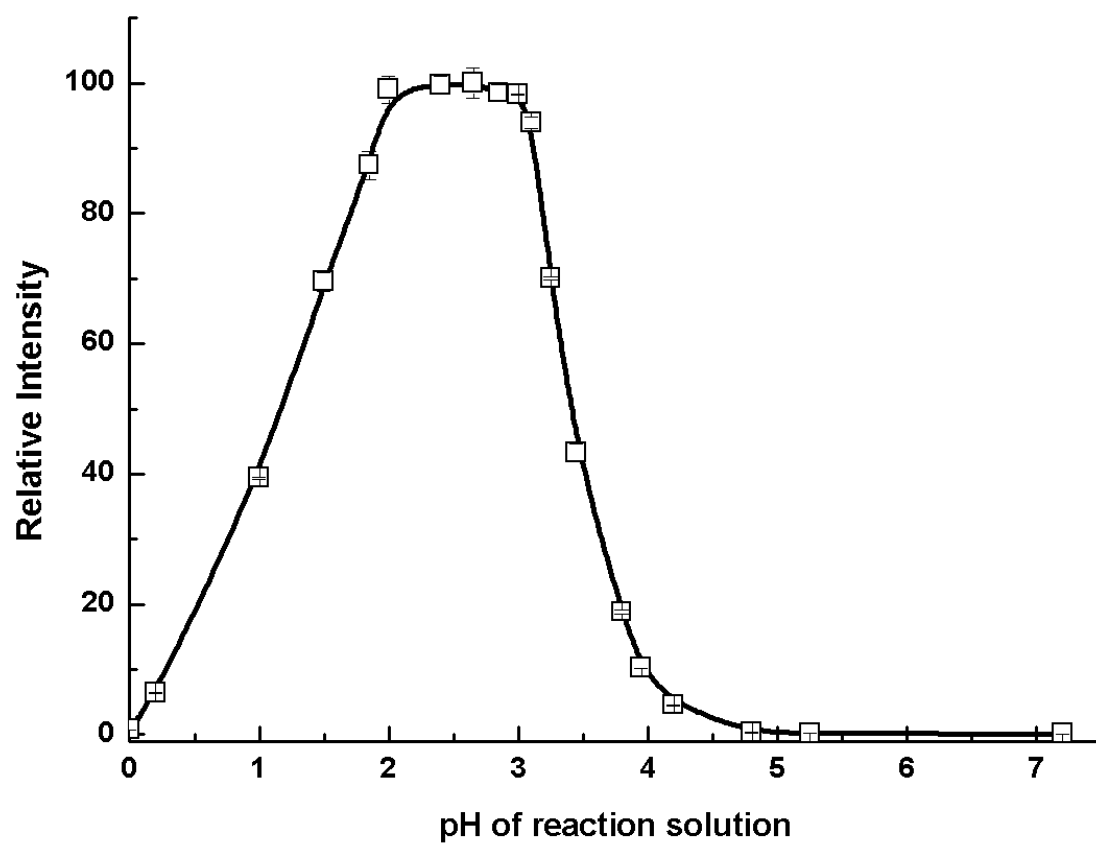


Figure 6. Effect of pH on the response from 100 $\mu\text{g L}^{-1}$ Fe(III) in 50 % (v/v) formic acid.

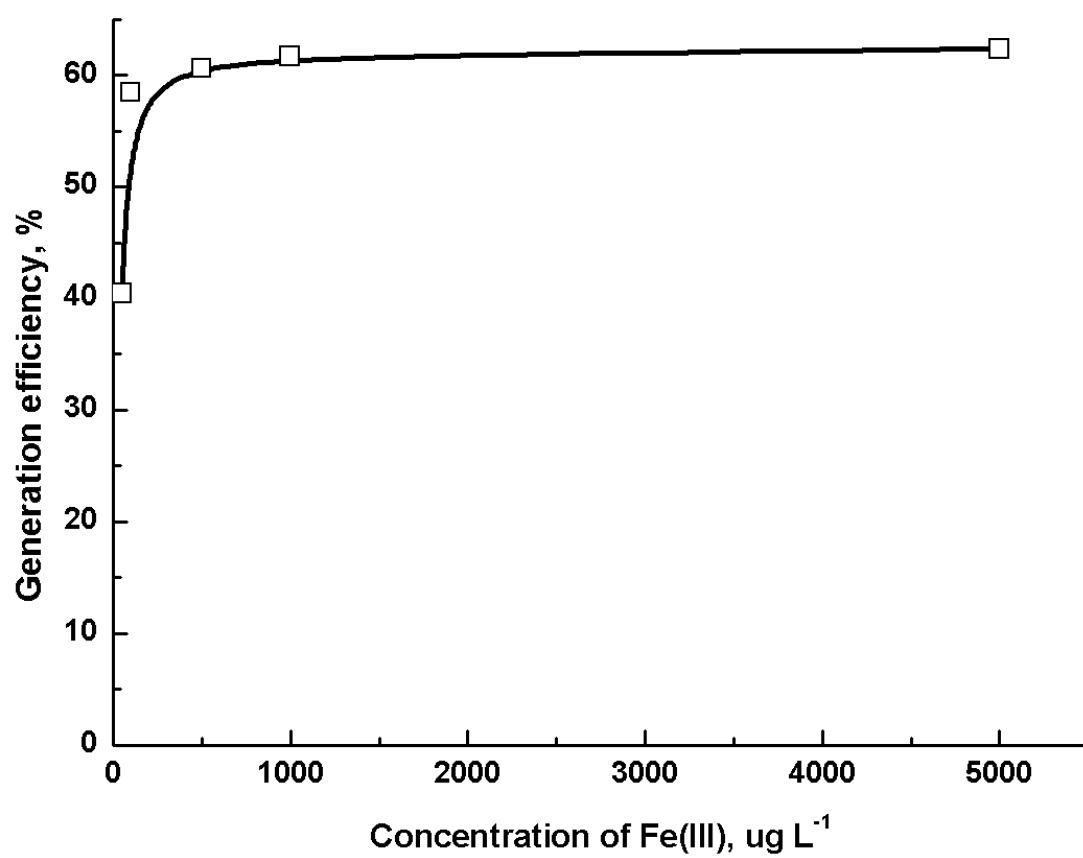


Figure 7. Efficiency of vapor generation.

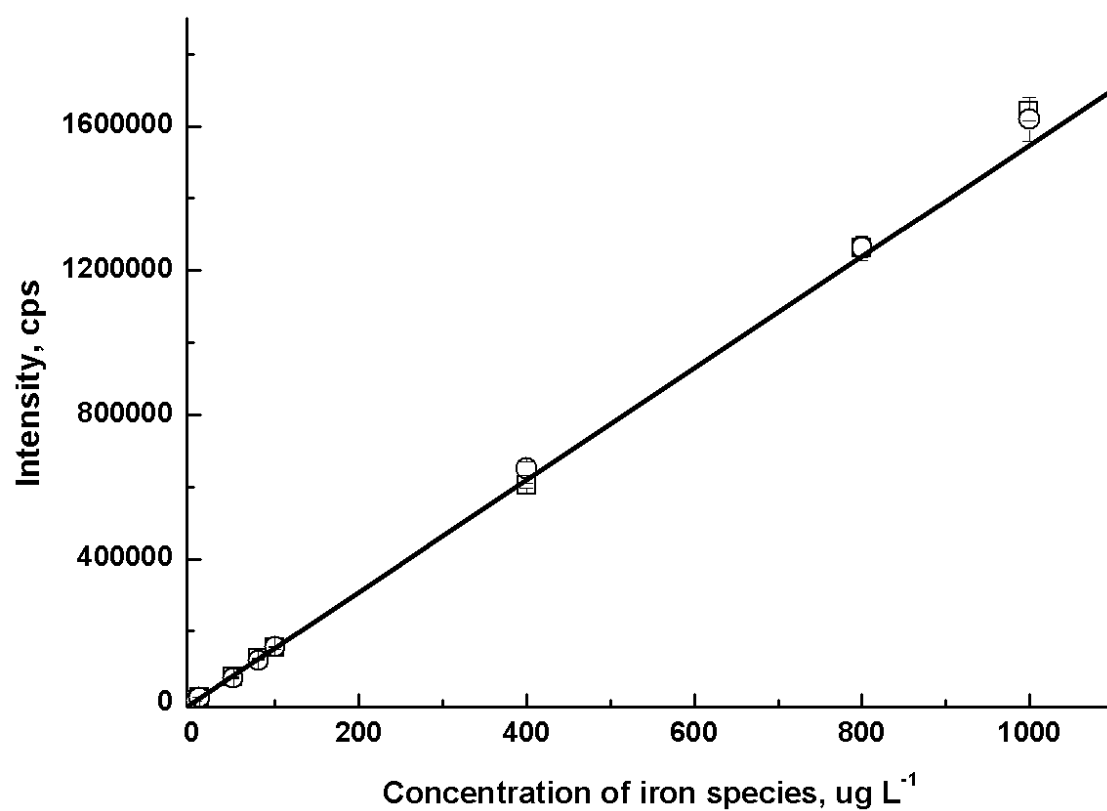


Figure 8. Typical calibration curves using PVG-ICP-OES obtained with \square Fe(II) and \circ Fe(III).